Conic optimisation for electric vehicle station smart charging with battery voltage constraints

Conic Optimisation for Electric Vehicle Station Smart Charging with Battery Voltage Constraints

Thomas Morstyn*, *Member, IEEE*, Constance Crozier, *Student Member, IEEE*, Matthew Deakin, *Member, IEEE*, and Malcolm D. McCulloch, *Senior Member, IEEE*

***Abstract*—This paper proposes a new convex optimisation strategy for coordinating electric vehicle charging, which accounts for battery voltage rise, and the associated limits on maximum charging power. Optimisation strategies for coordinating electric vehicle charging commonly neglect the increase in battery voltage which occurs as the battery is charged. However, battery voltage rise is an important consideration, since it imposes limits on the maximum charging power. This is particularly relevant for DC fast charging, where the maximum charging power may be severely limited, even at moderate state of charge levels. First, a reduced order battery circuit model is developed, which retains the nonlinear relationship between state of charge and maximum charging power. Using this model, limits on the battery output voltage and battery charging power are formulated as second-order cone constraints. These constraints are integrated with a linearised power flow model for three-phase unbalanced distribution networks. This provides a new multi-period optimisation strategy for electric vehicle smart charging. The resulting optimisation is a second-order cone program, and thus can be solved in polynomial time by standard solvers. A receding horizon implementation allows the charging schedule to be updated online, without requiring prior information about when vehicles will arrive.**

***Index Terms*—Battery modelling, DC fast charging, electric vehicle, second-order cone programming, smart charging.**

I. Introduction

THIS paper proposes a new optimisation strategy for coordinating electric vehicle charging in distribution networks. The proposed strategy accounts for battery voltage rise, and the associated limits on maximum charging power, while retaining a computationally scalable formulation.

Bloomberg estimates that electric vehicles will make up 55% of new global car sales and 33% of cars on the road by 2040 [1]. Electric vehicle adoption is being driven by the falling costs of lithium-ion batteries, and by government policies aiming to address air quality in cities and decarbonisation [2].

Without active coordination, electric vehicle charging is expected to require costly reinforcements of power system infrastructure. For example, it has been estimated that in the United Kingdom (UK), converting private vehicles to electric would increase peak demand by approximately 33% [3]. In addition, the My Electric Avenue project estimated that transport electrification would require reinforcements for around 32% of UK low voltage distribution feeders, even if only low power (3.5 kW) home charging is considered [4].

Currently, most electric vehicle chargers use a constant current–constant voltage (CC–CV) charging profile [5]. Under CC–CV charging, a battery is charged at its maximum current limit, until it reaches its maximum voltage limit. Once the voltage limit is reached, it is maintained by gradually reducing the charging current. CC–CV charging maximises the charging speed of a battery given a current limit and voltage limit specified by the manufacturer.

CC–CV charging results in varying upstream power demand, with a peak in demand just before the CV region is reached [6]. This is a challenge for electric vehicle chargers that are limited by an upstream power limit. For electric vehicle chargers with an individual upstream power limit, constant power–constant voltage (CP–CV) charging can be used [7][1]. In this case, the electric vehicle is charged according to the upstream power limit, until the maximum voltage limit is reached.

When groups of vehicles are charged at a site with a shared maximum power limit, a smart charging strategy is needed to coordinate the charging times and powers of the electric vehicles, so that the maximum power limit is not violated [8]. Smart charging strategies are also relevant for groups of electric vehicles embedded within a distribution network, where charging needs to be coordinated to prevent network constraints from being violated [9].

Electric vehicle smart charging strategies can be broadly divided into the following categories:

1) Convex optimisation strategies, which use a linearised battery state of charge model [10]–[18].
2) Non-convex optimisation strategies, which use a nonlinear battery state of charge model [19], [20].
3) Problem-specific heuristic strategies, including rule-based control [21], fuzzy expert systems [22] and stochastic algorithms [23].
4) Metaheuristic strategies, including particle swarm optimisation [24], [25], ant colony optimisation [26] and

This work is supported by the Engineering and Physical Sciences Research Council (project references EP/S000887/1 and EP/S031901/1), Innovate UK (project reference 104229) and the Oxford Martin Programme on Integrating Renewable Energy.

T. Morstyn, C. Crozier and M. D. McCulloch are with the Department of Engineering Science at the University of Oxford, Oxford OX1 2JD, United Kingdom.

M. Deakin is with the School of Engineering at Newcastle University, Newcastle upon Tyne, NE4 5TG, United Kingdom.

*Corresponding author, thomas.morstyn@eng.ox.ac.uk.

[1]It should be noted that although related, constant current battery charging and constant power battery charging are separate concepts to constant current loads and constant power loads from power system analysis. In particular, they refer to the charging current/power of the battery rather than the current/power drawn from the network.

evolutionary algorithms [27].

A common approach to obtain a computationally scalable optimisation problem for electric vehicle smart charging is to use a linear model for the relationship between battery charging power and state of charge [10]–[18]. Generally, this allows smart charging to be formulated as a convex linear program (LP), for which fast and robust solvers are readily available [28] (e.g. to achieve objectives such as maximising energy delivered to vehicles, or minimising peak demand). Linear battery models can be combined with a convex power flow model to incorporate electric vehicle charging into strategies for distribution network management [10].

A limitation of using a linear battery model is the implicit assumption that battery voltage remains constant. In reality, battery voltage increases at higher state of charge levels, and at higher charging powers [29]. An important implication is that at high state of charge levels, adhering to the battery voltage limit specified by the manufacturer will constrain the maximum charging power [30]. Optimisation strategies based on a linear battery model are suitable while batteries are charged in the CP region. However, once batteries reach the CV region, a smart charging strategy that does not model battery voltage rise will overestimate upstream power demand, and will underestimate the time required to reach full charge.

In [31], the nonlinear relationship between battery state of charge and maximum charging rate is identified as an underexplored aspect of electric vehicle charge scheduling. In [32], the impact of CC–CV electric vehicle charging on distribution network voltages is investigated considering nonlinear battery models, but coordinated scheduling is not considered. Optimal charge scheduling across multiple vehicles, considering their nonlinear battery characteristics, can be achieved using dynamic programming [19]. However, the computational complexity grows exponentially with the number of storage systems, limiting scalability [33]. Heuristic approaches have been proposed to find approximate solutions to nonlinear smart charging problems, including rule-based control [21], fuzzy expert systems [22], particle swarm optimisation [24], [25], ant colony optimisation [26] and evolutionary algorithms [27]. Limited scalability with increasing problem dimension remains a concern for heuristic strategies [34]. In [20], smart charging for an electric vehicle fleet is formulated as a mixed-integer nonlinear program, and solved using an iterative cutting-plane algorithm. The strategy accounts for the nonlinear relationship between battery state of charge and maximum charging power, but does not address internal battery resistance and charging losses. The smart charging strategy in [23] uses a stochastic algorithm to approximately flatten load between vehicles with fixed charging profiles that can be scheduled in time, but not reshaped or interrupted. However, this does not consider the potential for controlling vehicle charging power.

The reduction in maximum charging power that occurs as battery state of charge increases is particularly relevant for DC fast charging, due to the high power levels involved. Currently, DC charging standards offer charging between 50 kW and 200 kW, and there is a trend towards higher power levels [35]. Revised Combined Charging System and CHAdeMO standards are under development, which aim to support 350 kW to 400 kW charging for 800 V to 1000 V battery vehicles [36]. It has been recognised that although a significant amount of electric vehicle charging can be completed at low power, DC fast charging is a critical component of transport electrification policies for overcoming both perceived and actual range barriers [37]. The importance of effectively utilising the power capacity of expensive DC fast charging infrastructure motivates need for computationally scalable electric vehicle smart charging strategies that can account for nonlinear battery characteristics.

In this paper, a novel convex formulation for the electric vehicle smart charging problem is proposed which accounts for the nonlinear relationship between battery voltage, state of charge and maximum charging power. Compared with standard convex strategies that rely on a linear battery model, the proposed strategy is able to schedule charging profiles across groups of vehicles that can be closely followed without violating battery voltage limits. This allows for improved utilisation of upstream network capacity, while the strategy remains computationally scalable. A reduced order nonlinear battery circuit model is developed, and using this model, limits on the battery voltage and charging power are formulated as second-order cone constraints. These constraints are integrated with a linearised power flow model for three-phase unbalanced distribution networks, to provide a new multi-period optimisation strategy for electric vehicle smart charging. The resulting optimisation is a second-order cone program (SOCP), and thus can be solved in polynomial time by standard solvers [38], [39]. A receding horizon implementation allows the charging schedule to be updated online, without requiring prior information about when vehicles will arrive. The advantages of the proposed SOCP are demonstrated by comparing it with an LP formulated using a linear battery model.

The rest of this paper is organised as follows. In Section II, the second-order cone constraints for battery voltage and charging power are derived. Section III presents an LP and the proposed SOCP for smart charging in unbalanced distribution networks. Section IV presents simulation results demonstrating the performance of the proposed smart charging strategy. Section V concludes the paper.

II. Battery Modelling

For the smart charging strategies considered in this paper, $\mathcal{V} = \{1, \ldots, N_v\}$ is the set of electric vehicles and $\mathcal{T} = \{t_0 + 1, \ldots, t_0 + T\}$ is the optimisation time horizon.

A standard linear discrete time battery state of charge model is given by [12],

$$s_i(t) = s_i(t-1) + \frac{\eta_{bi}\Delta_{\mathcal{T}}}{\tilde{v}_{oi}C_{bi}} p_{oi}(t), \text{ for } p_{oi}(t) \geq 0. \quad (1)$$

For vehicle $i \in \mathcal{V}$ and optimisation interval $t \in \mathcal{T}$, $s_i(t)$ is the state of charge (ratio between 0 and 1), $p_{oi}(t)$ is the charging power (W), C_{bi} is the battery charge capacity (As), $\tilde{v}_{oi}$ is the nominal battery DC output voltage (V), η_{bi} is the nominal battery charging efficiency (ratio between 0 and 1) and $\Delta_{\mathcal{T}}$ is the optimisation interval duration (s).

The linear model does not account for the battery voltage increasing with state of charge and at higher charging powers.

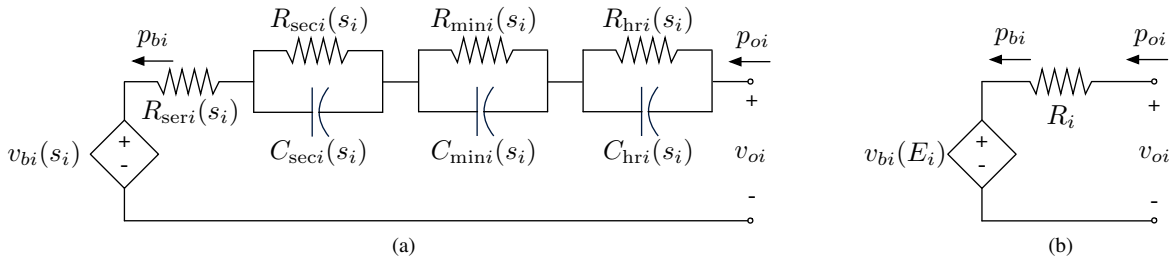

Fig. 1. (a) The multi-timescale nonlinear battery circuit model from [40]. The open circuit voltage v_{bi} and R, C values are 6th order logarithmic-polynomial functions of the state of charge s_i (ratio between 0 and 1). v_{oi} is the output voltage at the DC terminals of the battery (V), p_{oi} is the charging power at the battery terminals (W) and p_{bi} is the internal charging power (W). (b) The proposed reduced order nonlinear circuit model. The open circuit voltage is a linear function of the stored energy E_i (Ws), and the output resistance R_i is a fixed value (Ω).

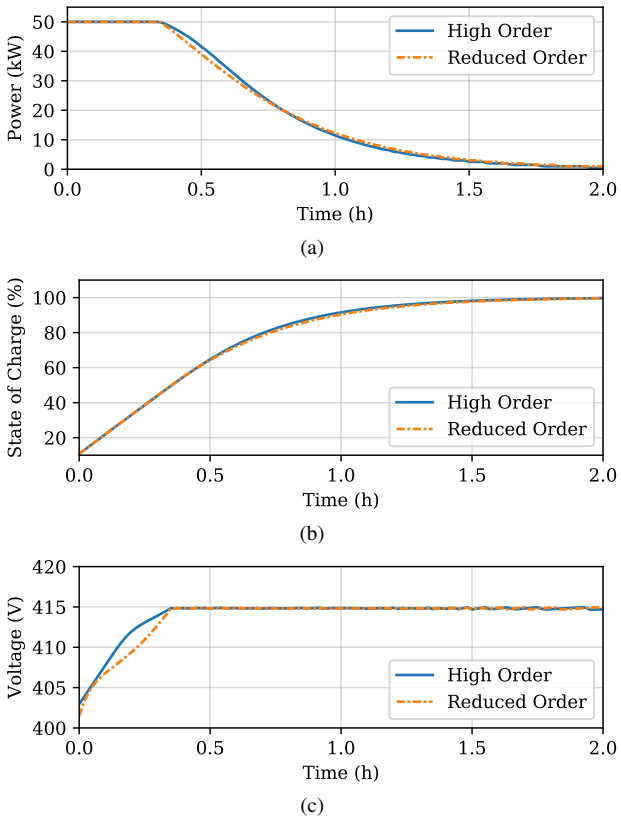

Fig. 2. Comparison between the high order battery model from [40] and the proposed reduced order model for a 40 kWh battery under CP–CV charging, with a power limit of 50 kW, a maximum voltage of 415 V and an initital state of charge of 10%. Profiles are shown for the (a) charging power, (b) state of charge and (c) battery output voltage.

To address this, nonlinear battery circuit models can be used for more accurate dynamic simulation. Battery circuit models include an inner voltage source to model the open circuit voltage, and series RC circuit elements to model the output impedance. These models incorporate the state of charge dependence of the open circuit voltage and output impedance by making the inner voltage source and circuit element values functions of the state of charge. In particular, [40] presents a multi-timescale validated model of this type with parameters for a lithium-ion battery cell used for electric vehicle applications. The model is shown in Fig. 1a. The open circuit voltage v_{bi} and R, C elements are each modelled as 6th order logarithmic-polynomial functions of the state of charge, with form,

$$x(s_i) = \exp\left[\sum_{k=1}^{6} \alpha_{xki} \log_e(s_i)^k\right] \tag{2}$$

Note that equivalent functions for the open circuit voltage and R, C elements, in terms of stored energy, E_i (Ws), can be obtained numerically.

The high order battery circuit model would give a non-convex optimisation formulation. To address this, the reduced order model shown in Fig. 1b is proposed. The open circuit voltage is modelled as a linear function of the stored energy,

$$v_{bi}(t) = a_{vi}\Delta_{\mathcal{T}} \sum_{\tau=t_0+1}^{t} p_{bi}(\tau) + v_{0i}, \tag{3}$$

$$v_{0i} = a_{vi}E_i(t_0) + b_{vi}. \tag{4}$$

p_{bi} is the charging power excluding losses (W), $E_i(t_0)$ is the initial stored energy (Ws) and a_{vi}, b_{vi} are model coefficients (V/Ws), (V).

Since the battery voltage limit is mainly of concern at the final state of charge, the output impedance is modelled by a single fixed resistance R_i (Ω), equal to the total series resistance at full charge. For the battery cell in [40], between 10% and 100% state of charge the total series resistance varies between 135 mΩ and 160 mΩ.

To compare the high order battery model and the proposed reduced order model, Fig. 2 shows output power, state of charge and output voltage profiles for each, for CP–CV charging of a 40 kWh battery with a maximum power limit of 50 kW. The battery is made up of 50 parallel $\times$ 100 series, 3.7 V nominal, 4.15 V maximum, 2.2 Ah cells, with parameters from [40]. Note that 50 kW is a common charging power for DC charging at CHAdeMO and Combined Charging System stations [41]. From 10% to 100% state of charge, the maximum absolute error between the high order and reduced order models is 2.65 kW for the charging power, 1.4% for the state of charge and 2.57 V for the battery output voltage.

If $\bar{v}_{oi}$ is the maximum output voltage at the DC terminals of the battery (V), then the maximum voltage constraint for $t \in \mathcal{T}$ is given by

$$\begin{aligned} v_{bi}(t) + R_i \tfrac{p_{bi}(t)}{v_{bi}(t)} \leq \bar{v}_{oi} \Leftrightarrow \\ v_{bi}^2(t) \leq \bar{v}_{oi} v_{bi}(t) - R_i p_{bi}(t). \end{aligned} \tag{5}$$

Since $v_{bi}(t) \geq 0$ and $\bar{v}_{oi} v_{bi}(t) - R_i p_{bi}(t) \geq 0$, this is equivalent to the following second-order cone constraint (see

Section 2.3 on hyperbolic constraints from [38]),

$$\begin{aligned}&\left\| \begin{matrix} 2(A_{ti}p_{bi} + v_{0i}) \\ (\bar{v}_{oi}A_{ti} + R_i e_t^\top)p_{bi} + \bar{v}_{oi}v_{0i} - 1 \end{matrix} \right\|_2 \\ &\quad \leq (\bar{v}_{oi}A_{ti} + R_i e_t^\top)p_{bi} + \bar{v}_{oi}v_{0i} + 1, \qquad (6) \\ &p_{bi} = [p_{bi}(t_0+1) \cdots p_{bi}(t_0+T)]^\top, \\ &A_{ti} = a_{vi}\Delta_{\mathcal{T}}[\mathbf{1}_{t-t_0}^\top \ \mathbf{0}_{T+t_0-t}^\top].\end{aligned}$$

$\mathbf{1}_x$ and $\mathbf{0}_x$ are vectors with length x and all entries equal to 1 and 0 respectively. e_t is a vector with a 1 at position $t - t_0$ and zeros elsewhere (i.e. $A_{ti}p_{bi} = a_{vi}\Delta_{\mathcal{T}} \sum_{\tau=t_0+1}^{t} p_{bi}(\tau)$ and $e_t^\top p_{bi} = p_{bi}(t)$).

For a maximum charging power $\bar{p}_{oi}$ (W), the power constraint for $t \in \mathcal{T}$ is given by

$$\begin{aligned}&p_{bi}(t) + R_i \tfrac{p_{bi}^2(t)}{v_{bi}^2(t)} \leq \bar{p}_{oi} \Leftrightarrow \\ &\qquad R_i p_{bi}^2(t) \leq v_{bi}^2(t)(\bar{p}_{oi} - p_{bi}(t)). \qquad (7)\end{aligned}$$

This is not a second-order cone constraint, but a conservative approximation can be obtained by replacing the right-hand side of the inequality with $v_{0i}v_{bi}(t)(\bar{p}_{oi} - p_{bi}(t))$, since $v_{0i} \leq v_{bi}(t)$. The new conservative constraint is,

$$\begin{aligned}&\left\| \begin{matrix} 2\sqrt{R_i}e_t^\top p_{bi} \\ e_t^\top p_{bi} - \bar{p}_{oi} + v_{0i}(A_{ti}p_{bi} + v_{0i}) \end{matrix} \right\|_2 \\ &\quad \leq \bar{p}_{oi} - e_t^\top p_{bi} + v_{0i}(A_{ti}p_{bi} + v_{0i}), \qquad (8)\end{aligned}$$

III. Electric Vehicle Smart Charging

In this section, optimisation strategies are formulated for electric vehicle smart charging at a set of charging stations within an unbalanced three-phase distribution network. For comparison, both an LP and the proposed SOCP are presented.

The objective of the charging stations is to maximise the energy that is delivered to electric vehicles, with priority given to vehicles with earlier arrival times. For commercial charging of private vehicles, arrival and departure times are likely to be unknown ahead of operation. To address this, the smart charging strategies here schedule charging based on the vehicles which have already arrived at a station, and are updated online with a receding optimisation horizon, so that the charging schedules are adjusted as new vehicles arrive. It is assumed that once vehicles arrive and plug-in, users provide their planned departure time (e.g. via a mobile app or parking meter). If vehicle arrival information was available ahead of operation, this information could be directly incorporated into the smart charging strategies.

In addition to the individual vehicle battery voltage and charging power constraints from Section II, the smart charging strategies need to consider the maximum import power of the stations and the distribution network voltage limits. For ease of presentation, it is assumed that the electric vehicles are charged at stations with balanced three-phase grid connections. The model can be straightforwardly generalised to the case where electric vehicles are charged with single phase connections. The proposed objective addresses fast charging within network and station constraints, but other objectives could be considered for different applications, such as minimising peak demand while meeting minimum vehicle energy requirements.

A. Distribution Network Model

The distribution network has buses $\mathcal{N} = \{0, \ldots, N_L\}$, where bus 0 is the slack bus, and the others are modelled as PQ buses. The network has three phases $\{a, b, c\}$, which may have unbalanced loads. Let $\mathcal{K}$ be the set of electric vehicle charging stations, and let $\mathcal{V}_k \subseteq \mathcal{V}$ be the subset of vehicles that charge at station $k \in \mathcal{K}$.

Electric vehicle charging station $k \in \mathcal{K}$ is located at bus $l_{\mathcal{V}_k} \in \mathcal{N} \setminus \{0\}$. To obtain approximate network voltage constraints for the smart charging strategies, the fixed point linearisation from [42] is applied for each interval of the optimisation time horizon, $t \in \mathcal{T}$. The network power flows are linearised around the power injections on each bus, excluding the electric vehicles.

Let $Y \in \mathbb{C}^{3(N_L+1)\times 3(N_L+1)}$ be the three-phase admittance matrix of the distribution network (Ω). The admittance matrix can be partitioned into $Y_{00} \in \mathbb{C}^{3\times 3}, Y_{0L} \in \mathbb{C}^{3\times 3N_L}, Y_{L0} \in \mathbb{C}^{3N_L\times 3}$ and $Y_{LL} \in \mathbb{C}^{3N_L\times 3N_L}$, where, $Y = \left[\begin{smallmatrix} Y_{00} & Y_{0L} \\ Y_{L0} & Y_{LL} \end{smallmatrix}\right]$.

For interval $t \in \mathcal{T}$, let the nominal wye and delta connected complex power injections (VA) be given by

$$s_l^Y(t) = [s_l^a(t)\ s_l^b(t)\ s_l^c(t)]^\top, \qquad (9)$$

$$s^Y(t) = [s_1^Y(t) \cdots s_{N_L}^Y(t)]^\top, \qquad (10)$$

$$s_l^\Delta(t) = [s_l^{ab}(t)\ s_l^{bc}(t)\ s_l^{ca}(t)]^\top \qquad (11)$$

$$s^\Delta(t) = [s_1^\Delta(t) \cdots s_{N_L}^\Delta(t)]^\top. \qquad (12)$$

The complex phase voltages for bus l are given by $v_l(t) = [v_l^a(t)\ v_l^b(t)\ v_l^c(t)]^\top$ (V). It is assumed that the slack bus has a fixed balanced voltage, $v_0/|v_0| = [1\ e^{-j\frac{2\pi}{3}}\ e^{j\frac{2\pi}{3}}]^\top$. For a set of nominal bus power injections $\tilde{s}^Y(t), \tilde{s}^\Delta(t)$, nominal bus voltages $\tilde{v}(t) = [\tilde{v}_1(t) \cdots \tilde{v}_{N_L}(t)]^\top$ for the linearisation can be calculated using the Z-Bus method [42]. This involves iteratively applying the following fixed-point equation to convergence,

$$\begin{aligned}\tilde{v}_{[k+1]}(t) = Y_{LL}^{-1}\big(&\text{diag}(\tilde{v}_{[k]}(t))^{-1}s^Y(t) \\ &+ H^\top \text{diag}(H\tilde{v}_{[k]}(t))^{-1}s^\Delta(t)\big) - Y_{LL}^{-1}Y_{L0}v_0, \qquad (13) \\ H = \text{blockdiag}&\left(\left[\begin{smallmatrix} 1 & -1 & 0 \\ 0 & 1 & -1 \\ -1 & 0 & 1 \end{smallmatrix}\right]\right).\end{aligned}$$

Let $p_{\mathcal{V}_k}(t)$ be the total load (W) for electric vehicle charging station $k \in \mathcal{K}$ at interval $t \in \mathcal{T}$. Let the maximum and minimum distribution network phase voltage magnitudes be given by $|\overline{v}|$ and $|\underline{v}|$ respectively ($|\text{V}|$). It is assumed that each charging station is wye connected and balanced, and that the charging stations have unity power factor. Therefore, approximate linear constraints on the phase voltage magnitudes are given by [42],

$$|\underline{v}|\mathbf{1}_{3N_L} \leq K_p^Y(t) \sum_{k\in\mathcal{K}} \frac{-p_{\mathcal{V}_k}(t)}{3} x_{\mathcal{V}_k} + |\tilde{v}(t)| \leq |\overline{v}|\mathbf{1}_{3N_L}, \qquad (14)$$

$$K_p^Y(t) = \text{diag}(|\tilde{v}(t)|)^{-1}\text{Real}\{\text{diag}(\tilde{v}(t)^*)Y_{LL}^{-1}\text{diag}(\tilde{v}(t)^*)^{-1}\},$$

$$x_{\mathcal{V}_k} = [\mathbf{0}_{3(l_{\mathcal{V}_k}-1)}^\top\ \mathbf{1}_3^\top\ \mathbf{0}_{3(N_L-l_{\mathcal{V}_k})}^\top]^\top.$$

$\tilde{v}(t)^*$ is the complex conjugate of the nominal bus voltages $\tilde{v}(t)$. $x_{\mathcal{V}_k}$ is a vector linking the load at charging station $k \in \mathcal{K}$ to the phases of bus $l_{\mathcal{V}_k}$. The matrix K_p^Y models the

relationship between wye-connected real power injections at each phase and the phase voltage magnitudes (|V|/W).

B. Linear Program

First, an LP for the proposed smart charging application is formulated based on the linear state of charge model in (1). This is similar to standard linear optimisation strategies from the literature, with two new application specific elements: (i) the objective function is designed for fast-charging vehicles at charging stations, prioritised according to arrival time; and (ii) network voltage constraints are included for a three-phase unbalanced distribution network. The LP is given by

$$\max_{p_o} \quad \sum_{t\in\mathcal{T}}\sum_{i\in\mathcal{V}}(T+t_0+1-\tau_{ai})\eta_{bi}p_{oi}(t) \tag{15a}$$

$$\text{s.t.} \quad \eta_{bi}\Delta_{\mathcal{T}}\sum_{t\in\mathcal{T}}p_{oi}(t)+E_i(t_0)\leq\overline{E}_i, \tag{15b}$$

$$0\leq\frac{n_{si}n_{pi}}{\eta_{ci}}p_{oi}(t)\leq\bar{p}_{ci}, \tag{15c}$$

$$p_{oi}(t)=0,\ t\in\mathcal{T}\setminus[\tau_{ai},\tau_{di}] \tag{15d}$$

$$p_{\mathcal{V}_k}(t)=\textstyle\sum_{i\in\mathcal{V}_k}\frac{n_{si}n_{pi}}{\eta_{ci}}p_{oi}(t), \tag{15e}$$

$$p_{\mathcal{V}_k}(t)\leq\bar{p}_{\mathcal{V}_k}, \tag{15f}$$

$$|\underline{v}|\mathbf{1}_{3N_L}\leq K_p^Y(t)\textstyle\sum_{k\in\mathcal{K}}\frac{-p_{\mathcal{V}_k}(t)}{3}x_{\mathcal{V}_k}+|\tilde{v}(t)|\leq|\bar{v}|\mathbf{1}_{3N_L}. \tag{15g}$$

Each electric vehicle $i\in\mathcal{V}$ has a battery pack, with n_{pi} parallel strings, each made up of n_{si} series cells. It is assumed that each pack has cell balancing electronics, so a single cell state of charge model can be used. The decision variables that are calculated by solving the LP are the battery cell charging powers for each vehicle, for each interval of the optimisation time horizon, $p_o=[p_{o1}\cdots p_{oN_v}]$, where $p_{oi}=[p_{oi}(t_0+1)\cdots p_{oi}(t_0+T)]^\top$ (W).

The objective function (15a) is formulated to maximise the energy delivered to the vehicles, weighted according to arrival time, so that vehicles that arrive earlier are given priority for charge scheduling. The energy delivered to vehicle i is weighted by $(T+t_0+1-\tau_{ai})$, where τ_{ai} is the arrival time interval. To prioritise charging according to departure time, $(T+t_0+1-\tau_{ai})$ can be replaced by $(\bar{\tau}_d+1-\tau_{di})$ in (15a), where $\bar{\tau}_d=\max\{\tau_{di}|i\in\mathcal{V}\}$. Constraint (15b) specifies that for each electric vehicle $i\in\mathcal{V}$, the total battery cell energy over the time horizon must remain below the maximum cell energy level $\overline{E}_i$ (Ws), where $E_i(t_0)$ is the initial cell energy (Ws).

Constraint (15c) limits the maximum charging power of each vehicle to the charger power limit $\bar{p}_{ci}$ (W). A fixed efficiency value, η_{ci} (ratio between 0 and 1), is used to model converter losses. Since power converter modelling is not the focus, the standard assumption of constant efficiency used for linear smart charging strategies is adopted (see e.g. [12]). In reality, converters have reduced efficiency away from a nominal operating point [43]. However, the high efficiency operating range is topology dependent and can be extended, for example by using parallel converter modules [44].

Electric vehicle $i\in\mathcal{V}_k$ arrives and plugs in at charging station $k\in\mathcal{K}$ at time interval τ_{ai}, and departs after time interval τ_{di}. Constraint (15d) ensures that the vehicles are only charged between their arrival and departure times. Constraint (15e) introduces variables, $p_{\mathcal{V}_k}(t), t\in\mathcal{T}$, which are equal to the total load of charging station k at each time interval. Constraint (15f) limits the total charging station load to $\bar{p}_{\mathcal{V}_k}$, and constraint (15g) addresses the distribution network phase voltage magnitude limits at each bus.

C. Second-Order Cone Program

The proposed SOCP for smart charging with battery voltage awareness is given by

$$\max_{p_b,p_o} \quad \textstyle\sum_{t\in\mathcal{T}}\sum_{i\in\mathcal{V}}(T+t_0+1-\tau_{ai})p_{bi}(t) \tag{16a}$$

$$\text{s.t.} \quad \Delta_{\mathcal{T}}\textstyle\sum_{t\in\mathcal{T}}p_{bi}(t)+E_i(t_0)\leq\overline{E}_i, \tag{16b}$$

(15c), (15d), (15e), (15f), (15g),

$$\left\|\begin{matrix}2(A_{ti}p_{bi}+v_{0i})\\(\bar{v}_{oi}A_{ti}+R_ie_t^\top)p_{bi}+\bar{v}_{oi}v_{0i}-1\end{matrix}\right\|_2 \leq(\bar{v}_{oi}A_{ti}+R_ie_t^\top)p_{bi}+\bar{v}_{oi}v_{0i}+1, \tag{16c}$$

$$\left\|\begin{matrix}2\sqrt{R_i}e_t^\top p_{bi}\\e_t^\top(p_{bi}-p_{oi})+v_{0i}(A_{ti}p_{bi}+v_{0i})\end{matrix}\right\|_2 \leq e_t^\top(p_{oi}-p_{bi})+v_{0i}(A_{ti}p_{bi}+v_{0i}). \tag{16d}$$

The SOCP has additional decision variables, $p_b=[p_{b1}\cdots p_{bN_v}]$, where $p_{bi}=[p_{bi}(t_0+1)\cdots p_{bi}(t_0+T)]^\top$ (W). The objective function (16a) and constraint (16b) are equivalent to (15a) and (15b) from the LP, but formulated in terms of the p_b variables, rather than the p_o variables. Constraints (15c)–(15g) are taken directly from the LP.

The reduced-order battery model from Section II is important for formulating the optimisation problem, since it allows the maximum voltage limits of the electric vehicle battery cells to be approximated by second-order cone constraints on the charging power decision variables. In particular, constraint (16c) limits the battery voltage of each vehicle $i\in\mathcal{V}$ to $n_{si}\bar{v}_{oi}$, and constraint (16d) enforces the relationship between the p_{bi} and p_{oi} variables.

D. Receding Horizon Implementation and Local Battery Voltage Regulation

It is assumed that the charging stations do not have prior information about when vehicles will arrive. To address this, the LP and SOCP smart charging strategies are implemented with a receding optimisation horizon [45]. Let $\hat{\mathcal{V}}$ be the set of vehicles which will arrive at a charging station at some point in time. At optimisation time interval t_0:

1) The optimisation problem ((15) or (16)) is formulated for t_0, based on $\mathcal{V}$, the set of vehicles which are at a charging station, where $\mathcal{V}=\{i\in\hat{\mathcal{V}}|\tau_{ai}\leq t_0\leq\tau_{di}\}$.
2) The optimisation problem is solved to obtain a set of charging power references $p_{oi}(t)$ for each electric vehicle, $i\in\mathcal{V}$ and each interval of the time horizon $t\in\mathcal{T}$.
3) For each electric vehicle $i\in\mathcal{V}$, the charging power reference for the current time interval $p_{oi}(t_0)$ is implemented for the duration of the optimisation interval $\Delta_{\mathcal{T}}$.
4) The optimisation horizon recedes to the next interval, $t_0\leftarrow t_0+1$.

TABLE I
CASE STUDY PARAMETERS

$\lvert\hat{\mathcal{V}}\rvert$	50	T	24	$\Delta_{\mathcal{T}}$	5 min
$\overline{E}_i$	8.14 Wh	C_{bi}	2.2 Ah	$\bar{v}_{oi}$	4.15 V
n_{si}	100	n_{pi}	25, 50 or 75	η_{bi}	0.91
η_{ci}	0.95	$\bar{p}_{ci}$	50 kW	$\bar{p}_{\mathcal{V}}$	120 kW
R_i	148 mΩ	a_{vi}	67.92 mV/Wh	b_{vi}	3.592 V
$\lvert\bar{v}\rvert$	1.05 pu	$\lvert\underline{v}\rvert$	0.95 pu	$\lvert v_0\rvert$	1.00 pu

Both the LP and the proposed SOCP provide charging power references $p_{oi}(t_0)$ for each electric vehicle, $i \in \mathcal{V}$, at each optimisation interval. The smart charging strategies are both formulated based on approximate models (the LP is based on the standard linear battery model in (1) and the proposed SOCP is based on the reduced-order battery circuit model in Fig. 1b). Since the smart charging strategies are based on approximate battery models, it is possible that directly implementing them would result in the battery voltage limits being violated. To address this, it is assumed that each vehicle charger has a local controller which operates at a fast timescale, and implements the charging power references from the optimisation strategy by adjusting the vehicle's charging power in 1% increments, ensuring the battery output voltage does not exceed the upper limit.

In this paper, it is assumed that the electric vehicle chargers have been designed with appropriate filters so that network harmonics are minimal and do not limit the number of vehicles which can be charged at once (see e.g. [46]). If this was not the case, an additional constraint could be added to the smart charging strategies to limit the maximum number of vehicles which could be charged simultaneously. Since the proposed SOCP smart charging strategy only adjusts the charging power references on a slow timescale (every 5 minutes) relative to the fundamental 50 Hz network frequency, it will not significantly impact the harmonics which would be present under a different smart charging strategy.

IV. RESULTS

Case study simulations are presented to demonstrate the operation of the proposed strategy for electric vehicle smart charging. The proposed SOCP (16) is compared with the LP (15) for scheduling multiple electric vehicles at a charging station, which is embedded within an unbalanced three-phase distribution network. Results are also included for the case without coordination, where vehicles operate under CC–CV charging, without considering the combined impact on the upstream power demand and network voltages.

The electric vehicles in the case study have a mix of 20, 40 and 60 kWh lithium-ion batteries, made up of 3.7 V nominal, 4.15 V maximum, 2.2 Ah cells. Verification of the impact the output power references generated by the LP and SOCP on battery state of charge and voltage is obtained by applying them to the high fidelity 6th order multi-timescale battery model (2) from [40], with a simulation time-step of 6 seconds. The impact on distribution network power flows and voltages are obtained using the nonlinear unbalanced three phase power flow Z-Bus method from [42]. The simulations

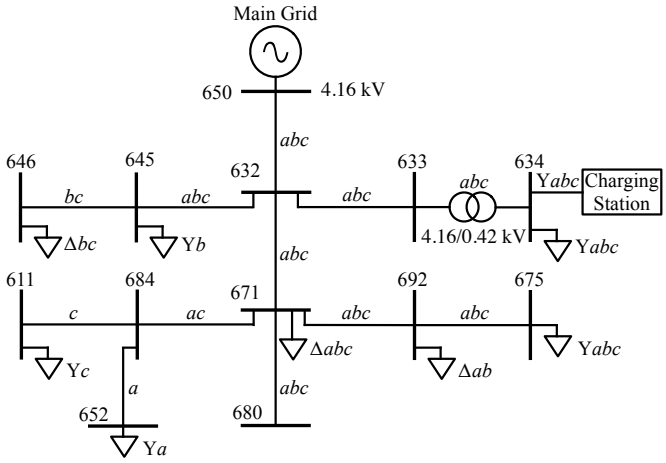

Fig. 3. The IEEE 13 Node Test Feeder which has been adapted for the case study. The connected phases for each line and load are indicated (e.g. abc for three-phase connection), as well as the connection configurations for the loads (Y for wye and Δ for delta).

were completed using Python. Table I provides the case study parameters.

Smart charging with the LP and the proposed SOCP are compared for an electric vehicle charging station embedded within a three-phase distribution network. The smart charging strategies are formulated to schedule individual charging power profiles for each electric vehicle at the station, subject to the vehicles' individual constraints, as well as collective constraints on the charging station's maximum power and the voltage limits throughout the distribution network. The objective of each smart charging strategy is to maximise the energy delivered to the vehicles, weighted so that vehicles with earlier arrival times have priority.

The electric vehicle charging station has a total maximum import limit of 120 kW. The station offers vehicles 50 kW DC charge points. 50 vehicles arrive between 6 am and 6 pm, and they each remain at the charging station between 15 minutes and 4 hours. Of the 50 vehicles, 20 have 20 kWh batteries, 20 have 40 kWh batteries and 10 have 60 kWh batteries. Vehicles arrive with state of charge levels between 10% and 40%. The arrival times, durations spent plugged-in and initial state of charge levels are generated randomly from uniform distributions. A longer optimisation horizon will increase performance, but also increases the computational burden. In [47], a horizon greater than the settling time of the plant under control is recommended. Based on the charging time observed in Fig. 2, a 2-hour duration optimisation horizon has been selected. 5-minute duration intervals are selected to match the resolution of the distribution network load data.

Fig. 3 shows the IEEE 13 Node Test Feeder [48], which has been adapted for the case study. The IEEE 13 Node Test Feeder is a three-phase 4.16 kV distribution network. It is appropriate that the charging station is placed at the distribution network level since standard distribution network transformers have power ratings between 100 kVA and 2.5 MVA [49]. The following changes have been made to the IEEE 13 Node Test Feeder: (i) The electric vehicle charging station

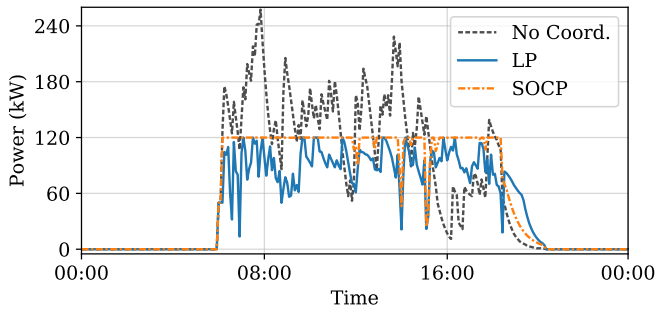

Fig. 4. The total charging power of the electric vehicle station, when vehicles operate individually under CC–CV charging without coordination, and when the vehicles are scheduled by the LP and the proposed SOCP. The 120 kW limit is not violated under either smart charging strategy. Without coordination the maximum power demand is 257 kW.

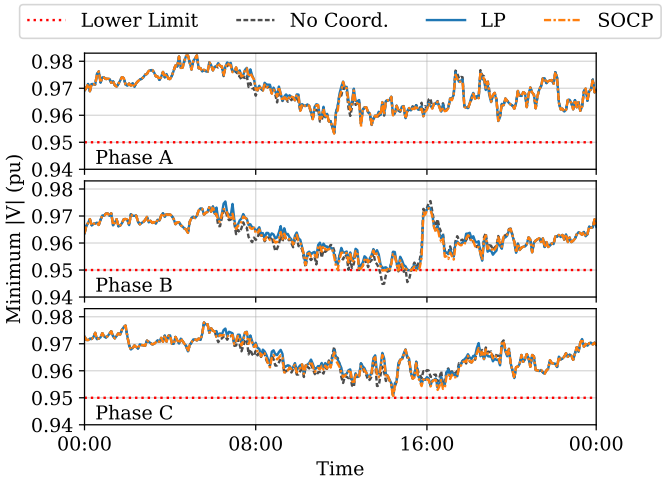

Fig. 5. The minimum phase voltage magnitudes across the distribution network buses, when vehicles operate individually under CC–CV charging without coordination, under the LP and under the proposed SOCP.

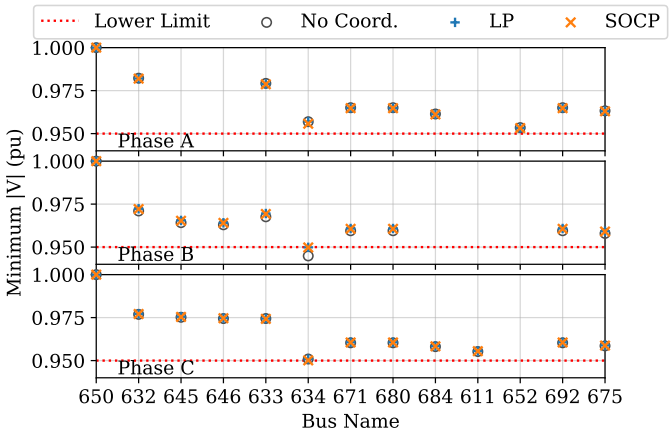

Fig. 6. The minimum phase voltage magnitudes for each distribution network bus over the case study, when vehicles operate individually under CC–CV charging without coordination, under the LP and under the proposed SOCP. (Note that not all buses have all three phases connected, as indicated by the missing values).

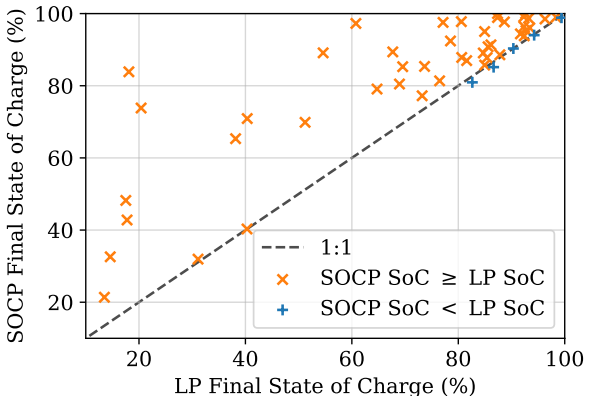

Fig. 7. The final state of charge reached by each of the 50 electric vehicles under the LP and the proposed SOCP.

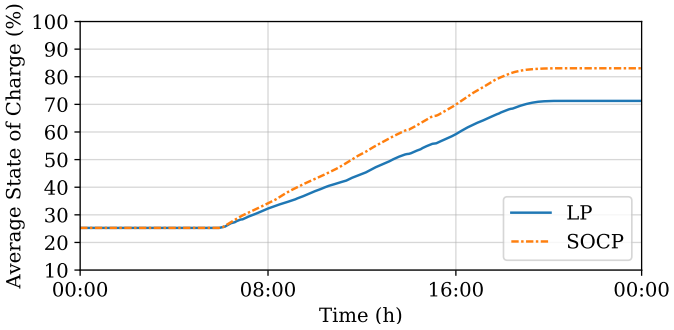

Fig. 8. The cumulative average state of charge of the 50 electric vehicles under the LP and the proposed SOCP.

has been added with a wye connection at bus 634. Bus 634 was selected since it is the only low voltage bus in the network. (ii) The loads have been replaced with 5-minute resolution 24-hour load profiles. Three-phase substation load data collected during August 2014 by the Customer Led Network Revolution trial was used for this purpose [50]. The total distribution network load across the three phases varies between 925 kW and 2250 kW, and the power factor varies between 0.88 and 0.97. The maximum real power load imbalance between any two phases is equal to 12% of the total load across the three phases. (iii) To demonstrate the ability of the proposed smart charging strategy to be used for voltage regulation, we have removed the voltage regulator normally between bus 650 and bus 632. For the case study, it has been assumed that the grid connected bus, bus 650, has a balanced fixed voltage with magnitude 1.00 pu, and that the distribution network has a lower phase voltage magnitude limit of 0.95 pu and an upper limit of 1.05 pu [51].

Fig. 4 shows the total charging power of the electric vehicle station, when vehicles operate individually under CC–CV charging without coordination, and when vehicles are scheduled by the LP and the proposed SOCP. CC–CV charging gives the fastest charging rate for each vehicle without violating their individual current limits and voltage limits. However, the combined power demand reaches 257 kW, which violates the shared 120 kW charging station power limit. Under the LP and the proposed SOCP, individual vehicle charging power references are calculated that respect both individual and shared constraints, and these references set the CP–CV charging power limit. This gives slower charging, but

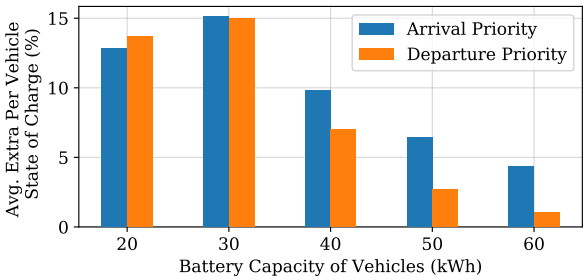

Fig. 9. The average additional per-vehicle final state of charge under the proposed SOCP compared with the LP, for cases with different sized vehicle batteries, and when charging is prioritised either based on vehicle arrival time or departure time.

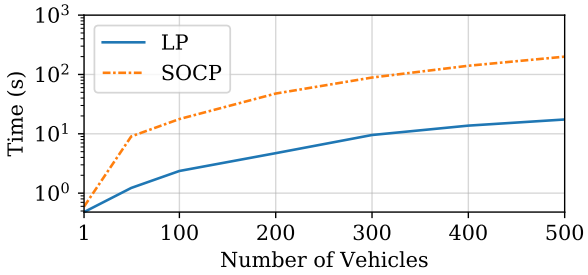

Fig. 10. The computation time for the LP and proposed SOCP, for problem instances with a 2-hour optimisation horizon, 5-minute intervals and different numbers of electric vehicles.

the total output power remains below the charging station's power limit. Compared with the SOCP, the LP results in a lower utilisation of the charging station power limit, since it does not account for battery voltage rise. For batteries with high state of charge levels, the LP schedules charging powers which need to be reduced to ensure the battery voltage limits are not violated. Considering the hours when vehicles are plugged in, the average utilisation of the charging station's 120 kW power limit is 70.3% under the LP and 87.4% under the proposed SOCP.

Since the distribution network does not have embedded generation, the lower voltage limit is of main concern. Fig. 5 shows the minimum phase voltage magnitudes across the distribution network buses, without coordination, under the LP and under the proposed SOCP. Fig. 6 shows the minimum phase voltage magnitudes over the case study for each of the distribution network buses. Without coordination, the phase B voltage reaches 0.945 pu, violating the 0.95 pu lower bound. Under the LP and the SOCP the lower voltage limits on phase B are reached, but not exceeded by more than 2×10^{-4} pu (these slight violations are due to the linearised power flow model).

Fig. 7 shows the final state of charge reached by each of the 50 electric vehicles prior to departure under the LP and the proposed SOCP, and Fig. 8 shows the cumulative average state of charge of the electric vehicles for each. The average final state of charge is 83.1% under the proposed SOCP, 11.8% higher than under the LP which gave a average final state of charge of 71.3%. In addition, 90% of the vehicles reach a higher individual final state of charge under the SOCP. Of the vehicles that finish with a lower final state of charge under the SOCP, their average final state of charge is only 0.8% less than under the LP. When the vehicles operate individually under CC–CV charging without coordination, the average final state of charge reached is 95.2% (12.1% higher than under the proposed SOCP). This comes at the cost of the power demand limit and network voltage limit violations shown in Fig. 4 and 5.

Additional studies were completed with all vehicles having either 20, 30, 40, 50 or 60 kWh batteries, and with the smart charging strategies prioritising vehicles according to arrival time, or modified to prioritise charging according to departure time. Fig. 9 shows the average additional per-vehicle final state of charge under the proposed SOCP compared with the LP for each case. The proposed SOCP is able to deliver more charge than the LP in all cases. The SOCP makes the most difference when the vehicles have 30 kWh batteries. Above 30 kWh, the battery voltage limits are reached at a higher state of charge, reducing the importance of accurate voltage modelling. Below 30 kWh, the total energy which needs to be delivered to the vehicles is reduced, which means that the performance of the LP is not impacted as much by its tendency to overestimate the power that can be delivered to vehicles with high state of charge.

Fig. 10 compares the computation time of the LP and the proposed SOCP for different sized problem instances up to 500 vehicles, solved using CPLEX running on a 2.2 GHz Intel Core i7 CPU with 8 GB of RAM. As expected, the computation time increases more quickly for the SOCP than the LP, but not at an exponential rate.

V. Conclusion

A new convex optimisation strategy for electric vehicle smart charging has been presented, which accounts for the nonlinear relationship between battery state of charge, voltage and maximum charging power. This is particularly important for coordinating DC fast charging, where the maximum charging power is limited by battery voltage constraints even at moderate state of charge levels. Using a reduced order nonlinear battery circuit model, the problem is formulated as a SOCP, which means it can be solved in polynomial time by standard solvers. The proposed strategy provides improved performance over a strategy which is formulated using a linear battery model, since it schedules reference charging profiles that can be closely followed without violating battery voltage limits. This is particularly valuable when coordinating vehicles that share an upstream power limit. A receding horizon implementation allows the charging schedule to be updated online as new vehicles arrive.

References

[1] C. McKerracher, "Electric Vehicle Outlook 2018," *Bloomberg New Energy Finance*, 2017, accessed Oct. 1 2018. [Online]. Available: bnef.turtl.co/story/evo2018?teaser=true

[2] C. W. Tessum, J. D. Hill, and J. D. Marshall, "Life Cycle Air Quality Impacts of Conventional and Alternative Light-Duty Transportation in the United States," *Proceedings of the National Academy of Sciences*, vol. 111, no. 52, pp. 18 490–18 495, 2014.

[3] C. Crozier, D. Apostolopoulou, and M. McCulloch, "Mitigating the Impact of Personal Vehicle Electrification: A Power Generation Perspective," *Energy Policy*, vol. 118, pp. 474–481, 2018.

[4] "My Electric Avenue - Summary Report," Tech. Rep., 2015, accessed Nov. 26 2018. [Online]. Available: http://myelectricavenue.info

[5] E. Inoa and J. Wang, "PHEV Charging Strategies for Maximized Energy Saving," *IEEE Transactions on Vehicular Technology*, vol. 60, no. 7, pp. 2978–2986, 2011.

[6] F. Marra, *et al.*, "Demand Profile Study of Battery Electric Vehicle Under Different Charging Options," in *IEEE Power and Energy Society General Meeting*, 2012, pp. 1–7.

[7] N. K. Poon, B. M. Pong, and C. K. Tse, "A Constant-Power Battery Charger with Inherent Soft Switching and Power Factor Correction," *IEEE Transactions on Power Electronics*, vol. 18, no. 6, pp. 1262–1269, 2003.

[8] R. R. Deshmukh and M. S. Ballal, "An Energy Management Scheme for Grid Connected EVs Charging Stations," *IEEE International Conference on Power, Instrumentation, Control and Computing*, pp. 1–6, 2018.

[9] K. Qian, C. Zhou, M. Allan, and Y. Yuan, "Modeling of load demand due to EV battery charging in distribution systems," *IEEE Transactions on Power Systems*, vol. 26, no. 2, pp. 802–810, 2011.

[10] S. Sojoudi and S. H. Low, "Optimal Charging of Plug-in Hybrid Electric Vehicles in Smart Grids," in *IEEE Power and Energy Society General Meeting*, 2011, pp. 1–6.

[11] Y. He, B. Venkatesh, and L. Guan, "Optimal Scheduling for Charging and Discharging of Electric Vehicles," *IEEE Transactions on Smart Grid*, vol. 3, no. 3, pp. 1095–1105, 2012.

[12] N. Chen, C. W. Tan, and T. Q. S. Quek, "Electric Vehicle Charging in Smart Grid: Optimality and Valley-Filling Algorithms," *IEEE Journal of Selected Topics in Signal Processing*, vol. 8, no. 6, pp. 1073–1083, 2014.

[13] T. Morstyn, A. Teytelboym, and M. D. McCulloch, "Matching Markets with Contracts for Electric Vehicle Smart Charging," in *IEEE Power & Energy Society General Meeting (PESGM)*, 2018, pp. 1–5.

[14] M. Liu, P. K. Phanivong, Y. Shi, and D. S. Callaway, "Decentralized Charging Control of Electric Vehicles in Residential Distribution Networks," *IEEE Transactions on Control Systems Technology*, pp. 1–16, 2017.

[15] J. Hu, S. You, M. Lind, and J. Ostergaard, "Coordinated Charging of Electric Vehicles for Congestion Prevention in the Distribution Grid," *IEEE Transactions on Smart Grid*, vol. 5, no. 2, pp. 703–711, 2014.

[16] J. Rivera, C. Goebel, and H. A. Jacobsen, "Distributed Convex Optimization for Electric Vehicle Aggregators," *IEEE Transactions on Smart Grid*, vol. 8, no. 4, pp. 1852–1863, 2017.

[17] L. Zhang, V. Kekatos, and G. B. Giannakis, "Scalable Electric Vehicle Charging Protocols," *IEEE Transactions on Power Systems*, vol. 32, no. 2, pp. 1451–1462, 2017.

[18] M. Liu, P. K. Phanivong, and D. S. Callaway, "Customer-and Network-Aware Decentralized EV Charging Control," in *IEEE Power Systems Computation Conference (PSCC)*, no. 1, 2018, pp. 1–7.

[19] Y. Levron, J. M. Guerrero, and Y. Beck, "Optimal Power Flow in Microgrids With Energy Storage," *IEEE Transactions on Power Systems*, vol. 28, no. 3, pp. 3226–3234, 2013.

[20] N. Korolko and Z. Sahinoglu, "Robust Optimization of EV Charging Schedules in Unregulated Electricity Markets," *IEEE Transactions on Smart Grid*, vol. 8, no. 1, pp. 149–157, 2017.

[21] Y. Cao, *et al.*, "An Optimized EV charging Model Considering TOU Price and SOC Curve," *IEEE Transactions on Smart Grid*, vol. 3, no. 1, pp. 388–393, 2012.

[22] E. Akhavan-Rezai, M. F. Shaaban, E. F. El-Saadany, and F. Karray, "Online Intelligent Demand Management of Plug-in Electric Vehicles in Future Smart Parking Lots," *IEEE Systems Journal*, vol. 10, no. 2, pp. 483–494, 2016.

[23] Lingwen Gan, Ufuk Topcu, and S. H. Low, "Stochastic Distributed Protocol for Electric Vehicle Charging with Discrete Charging Rate," in *IEEE Power and Energy Society General Meeting*, 2012, pp. 1–8.

[24] J. Soares, Z. Vale, B. Canizes, and H. Morais, "Multi-Objective Parallel Particle Swarm Optimization for Day-Ahead Vehicle-to-Grid Scheduling," *IEEE Symposium on Computational Intelligence Applications in Smart Grid, CIASG*, vol. 2012, pp. 138–145, 2013.

[25] K. Liu, C. Zou, K. Li, and T. Wik, "Charging Pattern Optimization for Lithium-Ion Batteries with an Electrothermal-Aging Model," *IEEE Transactions on Industrial Informatics*, vol. 14, no. 12, pp. 5463–5474, 2018.

[26] Z. Moghaddam, I. Ahmad, D. Habibi, and Q. V. Phung, "Smart Charging Strategy for Electric Vehicle Charging Stations," *IEEE Transactions on Transportation Electrification*, vol. 4, no. 1, pp. 76–88, 2017.

[27] S. Detzler and S. Karnouskos, "A Model and an Evolutionary Algorithmic Approach Towards Optimization of Electric Vehicle Fleet Charging," *International Symposium on Smart Electric Distribution Systems and Technologies*, pp. 20–25, 2015.

[28] S. Boyd and L. Vandenberghe, *Convex Optimization*. Cambridge: Cambridge University Press, 2004.

[29] S. Rajagopalan, *et al.*, "Fast Charging: An In-Depth Look at Market Penetration, Charging Characteristics, and Advanced Technologies," in *World Electric Vehicle Symposium and Exhibition (EVS27)*, 2013, pp. 1–11.

[30] P. H. Notten, J. H. H. Veld, and J. R. Van Beek, "Boostcharging Li-ion batteries: A Challenging New Charging Concept," *Journal of Power Sources*, vol. 145, no. 1, pp. 89–94, 2005.

[31] Q. Wang, X. Liu, J. Du, and F. Kong, "Smart Charging for Electric Vehicles: A Survey From the Algorithmic Perspective," *IEEE Communications Surveys & Tutorials*, vol. 18, no. 2, pp. 1500–1517, 2016.

[32] A. M. Haidar and K. M. Muttaqi, "Behavioral Characterization of Electric Vehicle Charging Loads in a Distribution Power Grid Through Modeling of Battery Chargers," *IEEE Transactions on Industry Applications*, vol. 52, no. 1, pp. 483–492, 2016.

[33] T. Morstyn, A. V. Savkin, B. Hredzak, and H. D. Tuan, "Scalable Energy Management for Low Voltage Microgrids Using Multi-Agent Storage System Aggregation," *IEEE Transactions on Power Systems*, vol. 33, no. 2, pp. 1614–1623, 2018.

[34] S. Chen, J. Montgomery, and A. Bolufé-Röhler, "Measuring the Curse of Dimensionality and its Effects on Particle Swarm Optimization and Differential Evolution," *Applied Intelligence*, vol. 42, no. 3, pp. 514–526, 2015.

[35] I. Vidanalage, B. Venkatesh, R. Torquato, and W. Freitas, "Scheduling of Electrical Vehicle Charging for a Charging Facility with Single Charger," *IEEE Electrical Power and Energy Conference, EPEC*, no. 2012, pp. 1–6, 2018.

[36] A. Meintz, *et al.*, "Enabling Fast Charging – Vehicle Considerations," *Journal of Power Sources*, vol. 367, no. 4, pp. 216–227, 2017.

[37] M. Neaimeh, *et al.*, "Analysing the Usage and Evidencing the Importance of Fast Chargers for the Adoption of Battery Electric Vehicles," *Energy Policy*, vol. 108, pp. 474–486, 2017.

[38] M. S. Lobo, L. Vandenberghe, S. Boyd, and H. Lebret, "Applications of Second-Order Cone Programming," *Linear Algebra and Its Applications*, vol. 284, no. 1-3, pp. 193–228, 1998.

[39] R. Y. Zhang, C. Josz, and S. Sojoudi, "Conic Optimization for Control, Energy systems, and Machine Learning: Applications and Algorithms," *Annual Reviews in Control*, vol. 47, pp. 323–340, 2019.

[40] Y. Cao, R. C. Kroeze, and P. T. Krein, "Multi-Timescale Parametric Electrical Battery Model for use in Dynamic Electric Vehicle Simulations," *IEEE Transactions on Transportation Electrification*, vol. 2, no. 4, pp. 432–442, 2016.

[41] M. C. Falvo, D. Sbordone, I. S. Bayram, and M. Devetsikiotis, "EV Charging Stations and Modes: International Standards," in *International Symposium on Power Electronics, Electrical Drives, Automation and Motion*, 2014, pp. 1134–1139.

[42] A. Bernstein, *et al.*, "Load Flow in Multiphase Distribution Networks: Existence, Uniqueness, Non-Singularity and Linear Models," *IEEE Transactions on Power Systems*, vol. 33, no. 6, pp. 5832–5843, 2018.

[43] K. N. Kumar and K. J. Tseng, "Efficiency Evaluation of Coordinated Charging Methods Used for Charging Electric Vehicles," *IEEE PES Innovative Smart Grid Technologies Conference Europe*, pp. 270–275, 2016.

[44] D. Christen, S. Tschannen, and J. Biela, "Highly Efficient and Compact DC-DC Converter for Ultra-Fast Charging of Electric Vehicles," *International Power Electronics and Motion Control Conference and Exposition*, pp. LS5d.3–1–8, 2012.

[45] T. Morstyn, B. Hredzak, R. P. Aguilera, and V. G. Agelidis, "Model Predictive Control for Distributed Microgrid Battery Energy Storage Systems," *IEEE Transactions on Control Systems Technology*, vol. 26, no. 3, pp. 1107–1114, 2018.

[46] J. Byrne-Finley, B. K. Johnson, H. Hess, and Y. Xia, "Harmonic Distortion Mitigation for Electric Vehicle Recharging Scheme," *North American Power Symposium (NAPS)*, pp. 1–7, 2011.

[47] D. Mayne, J. Rawlings, C. Rao, and P. Scokaert, "Constrained Model Predictive Control: Stability and Optimality," *Automatica*, vol. 36, no. 6, pp. 789–814, 2000.

[48] K. P. Schneider, *et al.*, "Analytic Considerations and Design Basis for the IEEE Distribution Test Feeders," *IEEE Transactions on Power Systems*, vol. 33, no. 3, pp. 3181–3188, 2018.

[49] "Power Engineering Guide," Siemens AG, Tech. Rep., 2017. [Online]. Available: new.siemens.com/global/en/products/energy/topics/power-engineering-guide.html
[50] "Dataset: Urban Distribution Substation Transformer, Thermal Dataset," *Customer-Led Network Revolution*, 2014, accessed 1 November 2018. [Online]. Available: networkrevolution.co.uk/project-library/dataset-urban-distribution-substation-transformer-thermal-dataset
[51] "Electric Power Systems and Equipment – Voltage Ratings (60 Hz) ANSI/NEMA C84.1," 2006. [Online]. Available: www.nema.org/Standards

Thomas Morstyn (S'14-M'16) received the BEng (Hon.) degree from the University of Melbourne in 2011, and the PhD degree from the University of New South Wales in 2016, both in electrical engineering.

He is an EPSRC Research Fellow with the Department of Engineering Science at the University of Oxford, and he is a fellow with the Oxford Martin Programme on Integrating Renewable Energy. His research interests include multi-agent control and market design for integrating distributed energy resources into power system operations.

Constance Crozier (S'16) received the M.Eng degree in general engineering, with a specialty in information engineering, from the University of Oxford in 2016. She is currently pursuing the Ph.D degree in electrical engineering at the same university.

Her current research interests include analysis and optimisation of electric vehicle charging in electricity distribution networks.

Matthew Deakin (S'15-M'20) received the M. Eng degree in Engineering Science in 2015 from the University of Oxford, UK, where he graduated with the top score in his cohort. He then obtained the D. Phil. (Ph.D.) degree in Engineering Science in 2019, also from the University of Oxford, during which time he held a Clarendon Scholarship.

He was a stipendiary lecturer at Christ Church, University of Oxford from 2017-2019. He is currently working as a postdoctoral research associate at Newcastle University, UK, with the Supergen Energy Networks hub. His current research interests include unbalanced distribution network analysis, smart grids and multi-vector systems.

Malcolm D. McCulloch (SM'89) received the B.Sc. (Eng.) and Ph.D. degrees in electrical engineering from the University of the Witwatersrand, Johannesburg, South Africa, in 1986 and 1990, respectively.

In 1993, he joined the University of Oxford, Oxford, U.K., to head up the Energy and Power Group, where he is currently an Associate Professor in the Department of Engineering Science. He is active in the areas of electrical machines, transport, and smart grids. His work addresses transforming existing power networks, designing new power networks for the developing world, developing new technology for electric vehicles, and developing approaches to integrated mobility.